3rd AIAA Flow Control Conference, Fluid Dynamics and Co-located Conferences,
5-8 June, San Francisco, California, USA
DOI:10.2514/6.2006-3492

Influence of Stochastic Estimation on the Control of Subsonic Cavity Flow – A Preliminary Study

M. Debiasi[*], J. Little[†], E. Caraballo[‡], X. Yuan[§], A. Serrani[**], J. H. Myatt[††], and M. Samimy[‡‡]

Gas Dynamics and Turbulent Laboratory; Collaborative Center for Control Science
GDTL/AARL, 2300 West Case Road
The Ohio State University, Columbus, Ohio 43235, USA

This work aims at understanding how the different elements involved in the feedback loop influence the overall control performance of a subsonic cavity flow based on reduced-order modeling. To this aim we compare preliminary and limited sets of experimental results obtained by modifying some relevant characteristics of the loop. Our results support the findings in the literature that use of quadratic stochastic estimation is preferable to the linear one for real-time update of the model parameters. They also seem to indicate the merit of using more than one time sample of the pressure for performing the real-time update of the model through stochastic estimation. The effect of using two different sets of pressure signals for the stochastic estimation also corroborates previous findings indicating the need for optimizing the number and the placement of the sensors used in the feedback control loop. Finally we observed that the characteristics of the actuator can alter significantly the overall control effect by introducing in the feedback loop additional, undesirable frequency components that are not modeled and hence controlled. A compensator for the actuator is currently being designed that will alleviate this problem thus enabling a clearer understanding of the overall control technique.

I. Introduction

Successful application of feedback control is widespread in many applications. Only in recent years has feedback control of aerodynamic flows received focused attention (e.g., Cattafesta et al., 1997; Gad-el-Hak, 2000; Williams, Fabris and Morrow, 2000; Kegerise, Cattafesta and Ha, 2002; Rowley and Williams, 2003; Cattafesta et al., 2003; Samimy et al., 2003; Siegel et al., 2003; Gerhard et al., 2003; Glauser et al., 2004; Tadmor et al., 2004). Open-loop flow control, which can be quite useful in many applications, lacks the responsiveness and flexibility needed for application in dynamic flight environments. In contrast, closed-loop flow control is well-suited to the successful management of these cases since it allows adaptability to variable conditions. In addition, closed-loop control shows the potential to significantly reduce power requirements in comparison to open-loop control strategies (Cattafesta et al., 1997). Unfortunately, the tools of classical control systems theory are not directly applicable to aerodynamics flows since such systems display spatial continuity and non-linear behavior while also posing formidable modeling challenges due to their infinite dimensionality, a complexity introduced by the Navier-Stokes equations. In order to design and successfully implement a closed-loop control strategy, it is necessary to obtain a reduced-order

[*] Post Doctoral Researcher, Dept. of Mechanical Eng., Member AIAA
[†] Grad. Student, Dept. of Mechanical Eng., Student Member AIAA
[‡] Grad. Student, Dept. of Mechanical Eng., Student Member AIAA
[§] Grad. Student, Dept. of Electrical and Computer Eng.
[**] Assistant Professor, Dept. of Electrical and Computer Eng., Member AIAA
[††] Senior Aerospace Engineer, AFRL/VACA, Senior Member AIAA
[‡‡] Professor, Dept. of Mechanical Eng., Director of GDTL, Associate Fellow AIAA, Corresponding author: samimy.1@osu.edu

dynamical model of the flow, which can capture the important dynamics of the flow and actuation while remaining sufficiently simple to allow its use in model-based feedback control design.

The flow over a shallow cavity - a configuration relevant to many practical applications that has been extensively studied in the literature - was selected as study case for developing advanced flow control techniques. This flow is characterized by a strong coupling between the flow dynamics and the flow-generated acoustic field that can produce self-sustained resonance known to cause, among other problems, store damage and airframe structural fatigue in weapons bays. A comprehensive review of this phenomenon and of various control and actuation strategies developed for its suppression is given in Cattafesta et al. (2003) and Rowley and Williams (2006).

While in recent years we have examined other approaches to cavity flow control (Debiasi et al., 2004; Efe et al., 2005; Yan et al., 2006), our primary objective from the onset has been the development of control techniques based on reduced-order models of the cavity flow (Samimy et al., 2004; Yuan et al., 2005; Caraballo et al., 2005 & 2006; Samimy et al. 2006). The approach we have followed in the development of such model is based on the proper orthogonal decomposition (POD) method. This technique relies on the energy-containing eddies in the flow that can be extracted using the spatial correlation tensor of the velocity field in the form of spatial eigenmodes called POD modes. These structures are the most dominant features in the flow and arguably are the only entities that can effectively be controlled. The dynamics of the flow are obtained when these modes are modulated by amplitude coefficients obtained by projecting the Navier-Stoke equations governing the flow onto the POD basis. This results in a set of non-linear ordinary differential equations, which we use for controller design. The equations are autonomous and not useful for controller design purposes since the controller input is not explicit. Consequently, they must be recast in a form expressing the control input explicitly so that a feedback controller can be designed using the tools of control theory (Efe et al., 2003; Caraballo et al., 2005).

Recently we have used POD technique along with the Galerkin project to develop a reduced-order model and a matching controller based on experimental measurement of a Mach 0.3 flow over a shallow cavity (Caraballo et al., 2005). This initial result was followed by additional models and controllers that, in some cases, proved very effective in reducing the cavity flow resonance (Caraballo et al., 2006 and Samimy et al. 2006). In all these cases, the feedback control loop has the same structure which comprises the elements depicted in Figure 1 that work in concert and influence each other and thus the overall control effect. Various elements of the loop can be configured according to different design choices and as a result a wide range of possibilities exists that can influence the final control performance. Among these are the selection of flow cases used to derive the reduced-order models, the number and location of the dynamic pressure transducers used, the order of the stochastic estimation and the number of time steps it utilizes, the controller design approach, and the characteristics of the actuator. For some of these design parameters, it is relatively clear to understand what are the optimal characteristics required to advance the overall performance of the system. For instance, the use of large bandwidth and fast time response requires an actuator transfer function devoid of significant magnitude and phase variations in the useful frequency range. However other design choices may not be so clear in general and require additional analytical and experimental investigation.

Thus the purpose of this work is to evaluate experimentally the effect of changing some of the aforementioned design options. More precisely we explored the merit of using a model based on the baseline (non-actuated) flow alone versus a model that combines the baseline flow and the same with an open-loop forcing that reduces the cavity resonance. We also explored the effect of using one or more time samples in both linear and quadratic stochastic estimation to capture richer dynamics of the flow.

The experimental results discussed in this work seem to confirm analogous observations by other groups and indicate that quadratic stochastic estimation is generally a better performer than the linear one, increasing the number of time steps used appears beneficial, it is important to optimize the number and location of the sensors used, and using combined models that include both baseline and actuated cases can reduce the sensitivity to various disturbances. We also verified the need of developing a compensator that optimizes the output of the actuator to reduce any distortion of the control effect.

In section 2 we will introduce the flow facility used in this work. In section 3 we present the POD and Galerkin methods adopted for deriving the reduced-order model. This is followed in section 4 by a discussion of the controller design process and of the stochastic estimation used for real-time estimation of the flow model variables directly

from dynamic surface pressure measurements. We will present and discuss the experimental results in section 5, followed by concluding remarks in section 6.

II. The experimental facility

In the following we provide a summary of the experimental facility and techniques used in this study and described in more detail in Debiasi and Samimy (2004), Caraballo et al. (2005 and 2006), and Little et al. (2006). It is a small-scale, optically accessible blow-down wind tunnel with a cavity recessed in the floor and spanning the width of the test section. The air is conditioned in a settling chamber to minimize free stream turbulence and directed to the 50.8 mm (2 in) by 50.8 mm (2 in) test section, Figure 2, through a contoured converging nozzle before exhausting into the atmosphere. The facility can be operated in the Mach number range 0.20 to 0.70. The focus of this work is on a shallow cavity with length 50.8 mm and depth of 12.7 mm (0.5 in) corresponding to a cavity aspect ratio, L/D, of 4.

The output of a Selenium D3300Ti compression driver is channeled to the cavity leading edge where it exits at an angle of 30^o with respect to the main flow through a 2-D slot of 1 mm height that spans the cavity width. The actuator signals are produced by a dSPACE 1103 DSP control board are amplified by a Crown D-150A amplifier. This arrangement provides zero net mass, non-zero net momentum flow for actuation, similar to that of a synthetic jet, with actuator flow to main flow momentum ratio in the range of 10^{-4} to 10^{-6}. Figure 3 shows the magnitude transfer function of the pressure fluctuations measured 4 mm upstream the exit slot. It can be clearly seen that the actuator output presents distinct frequency peaks in the operating range of the compression driver. This characteristic can influence the overall performance of the controller as it will be discussed in section V.

The planar snapshots of the velocity field, required for the development of the low dimensional model, are acquired using a two-component LaVision particle image velocimetry (PIV) system. The flow is seeded with oil particles by using a 4-jet atomizer upstream of the stagnation chamber. This location allows homogenous dispersion of the particles throughout the test section. The images corresponding to the two pulses from a dual-head Spectra Physics PIV-400 Nd:YAG laser operating at the 2^{nd} harmonic (532 nm) were acquired by a 2000 by 2000 pixel CCD camera equipped with a 90 mm macro lens with a narrow band-pass optical filter. The PIV image processing provides a velocity vector grid of 128 by 128 over the approximate measurement domain of 50.8 mm (2 in) by 50.8 mm (2 in) on the x-y plane passing through center of the cavity, which translates to velocity vectors separated by approximately 0.4 mm.

Flush-mounted Kulite transducers are placed at various locations on the walls of the test section for dynamic pressure measurements, Figure 4. The transducers have a flat frequency response up to about 50 kHz, are powered by a dedicated signal conditioner, and their signals are band-pass filtered between 100 Hz and 10 kHz. For state estimation, dynamic pressure measurements are recorded simultaneously with the PIV measurements. In the current study, 1000 PIV snapshots are recorded for each flow/actuation condition explored. The PIV snapshots with a sampling rate of a few Hz are time-uncorrelated. For each PIV snapshot, 128 samples from the laser Q-switch signal and from each of the pressure transducers 1-6 of Figure 4 are acquired at 50 kHz. The simultaneous sampling of the laser Q-switch signal and the pressure signals allows the identification of the section of pressure time traces corresponding to the instantaneous velocity field. Additional recordings of 2^{18} points are acquired at 200 kHz and converted to non-dimensional pressure referenced to the commonly used value of 20 μPa. Short-time Fourier transform (STFT) is utilized to provide information on the time evolution of the frequency content of the unsteady pressure signal and spectra are obtained by averaging the corresponding spectrograms, Little et al (2006).

For closed-loop control of the flow, a dSPACE 1103 DSP board connected to a Dell Precision Workstation 650 is used. This system utilizes four independent, 16-bit A/D converters each with 4 multiplexed input channels and allows simultaneous acquisition and control processing of 4 signals and almost simultaneous, due to multiplexing, acquisition and processing of additional signals at a rate up to 50 kHz per channel to produce at the same rate a control signal from a 14-bit output channel.

III. Reduced-order Modeling

The primary focus of our research has been the development of tools and procedures for feedback control based on reduced-order models (Samimy et al. 2004, Caraballo et al. 2004 and Yuan et al. 2005), as it enables the application of control theory tools. The procedure adopted comprises a series of mathematical tools developed by the fluid dynamics community over several decades for the study of various aspects of turbulent flows.

The reduced-order model is derived by using the POD and the Galerkin projection methods to obtain the flow model, which consists of a set of ordinary nonlinear differential equations. These equations govern the time evolution of the POD modes. These two steps will briefly be discussed in this section.

A. Proper Orthogonal Decomposition Technique

In this work the snapshot POD method, introduced by Sirovich (1987), is used to obtain the spatial modes from the PIV images of the cavity flow. The u and v components of the fluctuating velocity field are used for the POD decomposition. The procedure followed here has been described in detail in our previous work (Caraballo et al. 2004 and 2006, and Samimy et al. 2006) and more details of the basics of the POD method can be found in Lumley (1967), Holmes et al. (1996) and Delville et al. (1998).

In the POD method, each of the fluctuating velocity components can be approximated as a linear expansion of spatial eigenvectors (or POD modes) each time-modulated by a corresponding modal amplitude. The number N of POD modes used depends on the nature of the problem and the purpose of the model.

We derived a POD representation of each of the flow conditions explored in this work from 1000 PIV snapshots of the corresponding flow field acquires as detailed in the previous section. The results indicate that the mean turbulence kinetic energy converges by using approximately 700 snapshots (Caraballo et al. 2006). Consequently all 1000 snapshots were used to obtain the POD modes. The method was applied to each of the individual flow condition as well as for combinations of the sets, as will be noted later.

B. Galerkin Projection

The second step is the reduction of the governing equations of the flow into a simplified system that can be solved in real time. This is achieved by projecting the Navier-Stokes equations onto the POD modes using Galerkin projection method. The compressible Navier-Stokes equations used are those derived in Rowley (2002) and details of the procedure are given in Samimy et al. (2004) and Caraballo et al. (2004).

The result of this procedure is a set of nonlinear ordinary differential equations for the mode amplitudes. (Caraballo et al 2005 and 2006). These equations are autonomous (the control input does not appear explicitly) and therefore not useful for controller design. In order to derive a model where the control input appears explicitly in the equations, a few methods are currently being explored. The one used in the present work is based on spatial sub-domain separation, Efe and Ozbay (2003) and Yan et al. (2006), which yields the following set of ordinary differential equations

$$\dot{a}(t) = F + Ga(t) + \begin{bmatrix} a^T(t)H^1 a(t) \\ \vdots \\ a^T(t)H^N a(t) \end{bmatrix} + B\Gamma(t) + \begin{bmatrix} \left(\overline{B}^1\Gamma(t)\right)^T a(t) \\ \vdots \\ \left(\overline{B}^N\Gamma(t)\right)^T a(t) \end{bmatrix}, \tag{3.1}$$

where the matrices of constant coefficients F, G, H^i, B and $\overline{B}^i$, $i=1,\ldots N$, are obtained from the Galerkin projection, and $\Gamma(t)$ is the control input applied at the forcing location, see Yuan et al. (2005). Equation (3.1) represents a model of the cavity flow in terms of the mode amplitudes $a_i(t)$ obtained with the POD method from time uncorrelated PIV snapshots.

IV. Model Simplification, Real-Time Estimate, and Controller Design

In this section we recall the additional steps used to further simplify the Galerkin system model (3.1), to employ it in real-time applications, and to design the corresponding model-based controller. The corresponding steps have been presented in details by the authors in previous works (Yuan et al., 2005 and Caraballo et al., 2005), and thus they will be only outlined here.

In this work, we have focused on two reduced-order flow models, MB and MBF, obtained as described in the previous sections and summarized in Table 1. The expression of the reduced-order flow model for both cases is the same non-linear state space model given by (3.1), with $N = 4$, whereas the numerical values of the model parameters obviously vary for each case.

Case	Forcing frequency, Hz	Comments
B	--	Baseline flow
F	3920	Open-loop forcing
MB	--	Control model based on B snapshots
MBF	--	Control model based on B and F snapshots

Table 1. Mach 0.3 flow baseline and open-loop forced flows and the models

A. Equilibrium analysis and model simplification

The constant term F is removed from the model (3.1) by means of the coordinate transformation $\tilde{a} = a - a_0$, where a_0 is the equilibrium point of (3.1). This has the effect of shifting the equilibrium point to the origin of the new coordinate, which facilitates controller design and stability analysis. The reader is referred to Caraballo et al. (2005) for a detailed description of the model simplification techniques.

B. Stochastic Estimation

In implementing the controller in the experiment, the variables involved in the simplified reduced-order model (4.1) must be related to variables that can be measured experimentally in real-time. A similar situation will also arise in any practical application. In our case real-time experimental data can only be obtained via surface measurements (e.g. surface pressure or surface shear stress measurements). We used stochastic estimation (SE) to correlate surface pressure measurements with the flow velocity data obtained via PIV. This technique, first proposed by Adrian (1979) as a method to extract coherent structures from a turbulent flow field, estimates flow variables at any location by using statistical information about the flow at a limited number ($\mathcal{L}$) of locations.

While linear stochastic estimation has often been used in the literature, Naguib et al. (2001) used both linear and quadratic terms for a more accurate estimate of the flow field from wall pressure measurements. For the cavity flow, this was confirmed by Ukeiley and Murray (2005) and by Caraballo et al. (2004). Similar observations were presented by Ausseur et al. (2006) for the case of flow-separation control. Thus, quadratic SE has been used in our recent works as well (Caraballo et al, 2005 and 2006).

However in the current analysis we observed that controllers based on the combination of the baseline flow with different open-loop forced flows produced very different changes of the cavity flow resonance even though, taken individually, the effects of the different open-loop forcing cases were very similar. This raised the suspicion that, among other causes, these differences could be caused by an "over-fitting" of the quadratic SE to each specific combined data set used for its derivation. That is, each quadratic SE is estimating very well the conditions corresponding to the data set used for its derivation but fails to provide an accurate estimation in other conditions, like the real-time experiments. Therefore we decided to evaluate if any benefit could be gained by using linear SE instead where richer dynamics of the flow were recovered by using one or more previous "time samples" of the

measured pressure fluctuations. For a fair and more complete comparison we also adopted the same multiple time samples approach to quadratic estimation as well.

As explained in Caraballo et al. (2005), by using fluctuating pressure measurements (that neglect the effect of mean flow) the SE naturally estimates the deviation from the equilibrium of each mode amplitude. For the case of linear SE, the expression used to estimate $\tilde{a}_i(t)$ at any time *t* is

$$\tilde{a}_i(t) = Cl_{iks}\, p'_k(t_s) \qquad i=1\ldots N, \quad k=1\ldots \mathcal{L}, \quad s=0, -1, -2, \ldots \qquad (4.1)$$

where *Cl* is the matrix of the estimation coefficients obtained by minimizing the average mean square error between the values of $\tilde{a}_i(t)$ obtained directly from the snapshots and the ones estimated with the pressure data recorded simultaneously to the snapshots as discussed in section 2. In our experimental setup, the real-time measurements of surface pressure used for estimation were obtained at the locations of transducers 1-6 in the cavity test section, Figure 2.

Similarly, for quadratic SE, the expression used to obtain the estimated values of $\tilde{a}_i(t)$ is

$$\tilde{a}_i(t) = Cq_{iks}\, p'_k(t_s) + D_{ikls}\, p'_k(t_s)\, p'_l(t_s) \qquad i=1\ldots N, \quad k, l=1\ldots \mathcal{L}, \quad s=0, -1, -2, \ldots \qquad (4.2)$$

where *Cq* and *D* are matrices of the estimation coefficients obtained as in the linear case. Additional details on the procedure to obtain the estimation matrices are available in Caraballo et al. (2004).

C. Linear quadratic state feedback control

A linear approximation at the origin of the simplified Galerkin model used for control design, is readily obtained as

$$\dot{\tilde{a}} = \tilde{G}\tilde{a} + \tilde{B}\Gamma\,. \qquad (4.3)$$

The eigenvalues of the matrix of the unforced system in equation (4.3) computed for the model MB and MBF are given in Table 2.

Model	Open loop eigenvalues	
MB	$\lambda_{1,2} = 1597 \pm 7023\mathrm{i}$	$\lambda_3 = -3652$, $\lambda_4 = -880$
MBF	$\lambda_{1,2} = 1397 \pm 7062\mathrm{i}$	$\lambda_3 = -2871$, $\lambda_4 = -697$

Table 2. Eigenvalues of the open-loop systems for each model

Similar to what discussed in Caraballo et al. (2006), the fourth-order Galerkin systems for both cases exhibit the same qualitative features (2 unstable complex conjugate eigenvalues plus 2 stable real eigenvalues) and as well as quantitative similarities. The presence of two unstable complex conjugate eigenvalues implies, as expected, that the flow corresponding to the equilibrium a_0 is an unstable solution for the Galerkin system, equation (3.1).

Since the pairs $(\tilde{G}, \tilde{B})$ for both cases are controllable, linear state-feedback design based on the linearized model, equation (4.3), offers a simple approach to the design of a controller for the simplified nonlinear model. The availability of real-time estimates (4.2) or (4.3) of the state of the model allows the use of linear state-feedback control to stabilize the origin of equation (4.3). This, in turn, yields a controller that locally stabilizes the origin of the nonlinear system; see Caraballo et al (2006). A convenient and well-established methodology for the state-feedback controller design is offered by linear-quadratic (LQ) optimal control. The LQ design computes the gain matrix *K* such that the state-feedback law

$$\Gamma(t) = -K\,\tilde{a}(t) \qquad (4.4)$$

minimizes a quadratic cost function as detailed in Caraballo et al. (2006). The minimization of the cost function results in asymptotic stabilization of the origin, while the control energy is kept small. The control gains for each model are given in Table 3.

Model	Controller gain K	α
MB	$[-56 \quad 8.8 \quad -417 \quad -12.8]$	0.265
MBF	$[17.6 \quad 209 \quad 11.6 \quad -147]$	0.5

Table 3. Controller gains

Further analysis and additional details on the effect of the control obtained above is presented in Caraballo et al. (2006).

V. Real-time control results

Before presenting the experimental results, it is worth summarizing the structure of the model-based controller thus derived. As depicted in Fig. 1, the stochastic estimation is a subsystem of the model-based controller. To protect the acoustic actuator, a saturation function is employed in cascade with the controller output. To prevent saturating the control input at all time, the controller is detuned using a constant scaling factor α, similarly to what has been presented in Caraballo et al. (2005). Thus the corresponding scaled control is in the form

$$\Gamma_\alpha(t) = -\alpha K \tilde{a}(t) \,. \tag{5.1}$$

Based on the figure of merit discussed next, for each control case the scaling factor α was progressively increased until one of the following occurred: a) no further reduction of the spectral peaks was observed, b) some peaks became as dominant as the reduced resonant tone, or c) the control signal reached the saturation limits.

In analyzing the experimental results obtained with the current control approach, sometimes we observed some differences between the spectral signatures of the different transducers in the test section, Fig. 4. This was not observed in our previous studies using optimal forcing frequency (Debiasi and Samimy, 2004) and parallel proportional with time delay control (Yan et al, 2006). Therefore in the current study we selected the average of the SPL spectra of transducers 1-6 used for control as a figure of merit for evaluating the overall control performance. We further verified that for the baseline cases and the controlled cases presented in previous works, the spectra obtained with this averaging compare well with the spectra from either sensor 5 or sensor 6 previously presented.

Figure 5 illustrates the effect of some changes in the SE of a controller derived for a model based on the baseline case B. More precisely it shows the effect of using an increasing number of time samples from each of the transducers 1-6 and the effect of increasing the order of the SE from linear (on the left) to quadratic (on the right). For both the linear and the quadratic cases a trend can easily be observed indicating a better spectral reduction of the cavity flow when a larger number of time samples is used in the SE. For a given number of time samples an improvement in spectral reduction is also observed by increasing the order of the SE from linear to quadratic. Unfortunately we could not verify the trends above for the case of quadratic SE with 4 time samples due to real-time performance limitations of our control board.

Of particular note is the performance achieved by the linear SE with 4 time samples, Fig. 5 (c) which reduced the resonant peak by 20 dB without raising the background broadband spectral components. This remarkable achievement ranks among the best we observed with our experimental setup. In all the cases of Fig. 5 additional peaks of varying magnitude are introduced with control. It is easy to observe that some of these peaks coincide with those of the frequency response of the pressure fluctuations near the actuation exit slot, Fig. 3. Thus the actuator introduces in the feedback loop some frequency components that, not being modeled and controlled, can become quite intense as is the case of peak “b” at about 1600 Hz in Fig. 5 (a) and (b).

In order to reduce the influence of actuation near the actuator exit and also to overcome the performance limitations encountered in implementing the case of quadratic SE with 4 time samples, we explored the effect of

using a reduced set of pressure transducers for SE. Correspondingly we dropped transducer 1, located at the cavity leading edge near the actuator exit, and also transducer 3, located at the cavity trailing edge and subject to high broadband loads. The corresponding results for the model based on the baseline case B are presented in Fig. 6 and parallel those of Fig. 5. The peak b induced by actuation has been reduced compared to the corresponding cases of Fig. 5. However other actuation peaks (a, c, and d) have been reinforced. Particularly troubling is the reinforcement of a component at 7 kHz that, almost negligible in Fig. 5, becomes more intense in Fig. 6 where it reached the level of 126 dB for linear SE with 4 time samples. The exact origin of this component (whose frequency actually coincides with that of a sharp drop in the frequency response of the actuator, Fig. 3) is not understood at this time.

The overall unexciting performance of the controller with the reduced set of transducers above is not completely surprising since it results from a rather heuristic reduction of the sensing locations operated without optimizing their placement in the test section. As suggested by other authors, Cohen et al. (2006) and Willcox (2006), a careful selection of the locations used for sensor placement plays a major role in the success of a control strategy based on reduced-order models. We are currently exploring some different and better configurations for sensor placement than the one presented in Fig. 4.

Notwithstanding these difficulties, Fig. 6 still indicates that increasing the order of the SE from linear to quadratic improves somewhat the overall control performance.

Figure 7 presents results for the composite model that combines the baseline and the forced cases and utilizes the full set of sensors of Fig. 4. Similar to Fig. 5, increasing the order of the SE from linear to quadratic produces control spectra with lower peaks. Analogous to the baseline model, an improvement is also observed when 2 time samples are used in both the linear and the quadratic SE. However, and different from Fig. 5, this trend is not confirmed with the use of 4 time samples in the linear case, Fig. 7 (c), and it could not be checked in the quadratic case, due to the aforementioned limitations of our control board.

This composite model appears to be slightly superior to the simpler baseline model when using linear SE with one or two time samples. In other conditions the two models have comparable performance. We also explored additional composite models (some also comprising a richer combination of forced cases) using the quadratic SE with one time sample. The results (not presented here) indicate that these composite models are equivalent or less effective than the simpler baseline model for reducing the Mach 0.3 cavity resonance. This behavior can be associated to our specific experimental setup or to the peculiar spatial sub-domain separation technique we use for the control input separation, and it will be further investigated in the future.

VI. Conclusions

In the recent past we made remarkable advances in developing a controller for subsonic cavity flow based on POD reduced order modeling. In order to make further progress, it is necessary to obtain a clearer understanding of how the different elements involved in the corresponding feedback loop work in concert and influence each other and thus the overall control effect. To this aim we compare preliminary, limited sets of experimental results obtained by modifying some relevant characteristics of the loop. We contrasted a model based exclusively on the baseline flow with a composite one based on the combination of the same baseline with an open-loop forcing. We also explored the effect of using linear and quadratic stochastic estimation for updating these models from pressure fluctuations measured by selected transducers. Finally we verified if any advantage exists in using one or more time samples of the pressure for better capturing the dynamics of the system.

The results obtained do not clearly support the superiority of the composite model. This finding can be associated to our experimental setup or to the spatial sub-domain separation technique used for the control input separation, and it will be further investigated in the future.

Our results confirm the findings in the literature that quadratic stochastic estimation is preferable to the linear one. They also seem to indicate the merit of using more than one time sample of the pressure for performing the real-time update of the model through stochastic estimation.

The effect of using two different sets of pressure signals for the stochastic estimation also corroborates previous studies indicating the need to optimize the number and the placement of the sensors used in the feedback control loop.

Finally we observed that the characteristics of the actuator can alter significantly the overall control effect by introducing in the feedback loop additional, undesirable frequency components that are not modeled and hence

controlled. A compensator for the actuator is currently being designed that will alleviate this problem thus enabling a clearer understanding of the overall control technique.

Acknowledgments

This work is supported in part by the AFRL/VA and AFOSR through the Collaborative Center of Control Science (Contract F33615-01-2-3154).

References

1. Adrian, R. J., "On the Role of Conditional Averages in Turbulent Theory," Turbulence in Liquids, Science Press, Princeton, 1979.
2. Ausseur, J.M., Pinier, J.T., Glauser, M.N., Higuchi, H. & Carlson, H., "Experimental Development of a Reducer-Order Model for Flow Separation Control," 2006, AIAA Paper 2006-1251.
3. Caraballo, E., Yuan, X., Little, J., Debiasi, M., Serrani, A., Myatt, J., and Samimy, M., "Further Development of Feedback Control of Cavity Flow Using Experimental Based Reduced Order Model," AIAA Paper 2006-1405, January 2006.
4. Caraballo, E., Yuan, X., Little, J., Debiasi, M., Yan, P. Serrani, A., Myatt, J., and Samimy, M., "Feedback Control of Cavity Flow Using Experimental Based Reduced Order Model," AIAA Paper 2005-5269, June 2005.
5. Caraballo, E., Malone, J., Samimy, M., and DeBonis, J., "A Study of Subsonic Cavity Flows - Low Dimensional Modeling," AIAA Paper 2004-2124, June 2004.
6. Cattafesta III, L. N., Williams, D. R., Rowley, C. W., and Alvi, F. S., "Review of Active Control of Flow-Induced Cavity Resonance," AIAA Paper 2003-3567, June 2003.
7. Cattafesta III, L.N., Garg, S., Choudhari, M., and Li, F., "Active Control of Flow-Induced Cavity Resonance", AIAA Paper 97-1804, June 1997.
8. Cohen, K., Siegel, S., and McLaughlin, T., "A Heuristic Approach to Effective Sensor placement for Modeling of a Cylinder Wake," *Computers & Fluids*, Vol. 35, 2006, pp. 103-120.
9. Debiasi, M. and Samimy, M., "Logic-Based Active Control of Subsonic Cavity Flow Resonance," *AIAA Journal*, Vol. 42, No. 9, pp. 1901-1909, September 2004.
10. Debiasi, M., Little, J., Malone, J., Samimy, M., Yan, P., and Özbay, H., "An Experimental Study of Subsonic Cavity Flow – Physical Understanding and Control," AIAA Paper 2004-2123, June 2004.
11. Delville, J., Cordier, L. and Bonnet, J.P., "Large-Scale-Structure Identification and Control in Turbulent Shear Flows," In Flow Control: Fundamentals and Practice, edited by Gad-el-Hak, M., Pollard A. and Bonnet, J., Springer-Verlag, 1998, pp. 199-273.
12. Efe, M., Debiasi, M., Yan, P., Özbay, H., and Samimy, M., "Control of Subsonic Cavity Flows by Neural Networks-Analytical Models and experimental Validation," AIAA Paper 2005-0294, January 2005.
13. Efe, M.Ö., and Özbay, H., "Proper Orthogonal Decomposition for Reduced Order Modeling: 2D Heat Flow," IEEE Int. Conf. on Control Applications (CCA'2003), June 23-25, Istanbul, Turkey, pp. 1273-1278, 2003
14. Gad-el-Hak, M., Flow Control – Passive, Active, and Reactive Flow Management, Cambridge University Press, New York, NY, 2000.
15. Glauser, M. N., Higuchi, H., Ausseur, J., and Pinier, J., "Feedback Control of Separated Flows (Invited)," AIAA Paper 2004-2521, June 2004.
16. Gerhard, J., Pastoor, M., King, R., Noack, B., Dillmann, A., Morzynski, M., and Tadmor, G., "Model-Based Control of Vortex Shedding using Low-Dimensional Galerkin Models," AIAA Paper 2003-4262, June 2003
17. Grove, J., Leugers, J., and Akroyd, G., "USAF/RAAF F-111 Flight Test with Active Separation Control", AIAA Paper
18. Holmes, P., Lumley, J.L., and Berkooz, G., "Turbulence, Coherent Structures, Dynamical System, and Symmetry," Cambridge University Press, Cambridge, 1996.
19. Kegerise, M., Cattafesta, L., and Ha, C., "Adaptive Identification and Control of Flow-Induced Cavity Oscillations," AIAA Paper 2002-3158, 2002.
20. Little, J., Debiasi, M., and Samimy, M., "Flow Structure in Controlled and Baseline Subsonic Cavity Flows," AIAA Paper 2006-0480, January 2006.
21. Lumley, J. "The Structure of Inhomogeneous Turbulent Flows", Atmospheric Turbulence and wave propagation. Nauca, Moscow. 1967 166-176.
22. Naguib, A., Wark, C. and Juckenhoefel, O., "Stochastic Estimation and Flow Sources Associated with Surface Pressure Events in a Turbulent Boundary Layer," *Physics of Fluids* 13, No. 9, 2001, pp.2611-2616.

23. Rowley, C., and Williams, D., "Dynamics and Control of High-Reynolds-Number Flow Over Open Cavities," *Annu. Rev. Fluid Mech*,. 38, 2006, pp. 251-276.
24. Rowley, C., and Williams, D., "Control of Forced and Self-Sustained Oscillations in the Flow Past a Cavity," AIAA Paper 2003-0008, 2003.
25. Rowley, C. W., "Modeling, Simulation and Control of Cavity flow Oscillations", Ph.D. thesis, California Institute of Technology. 2002.
26. Samimy, M., Debiasi, M., Caraballo, E., Serrani, A., Yuan, X., Little, J., and Myatt, J. H., "Reduced-order Model-based Feedback Control of Subsonic Cavity Flows – An Experimental Approach," Conference on active flow control, Germany, September 2006
27. Samimy, M., Debiasi, M., Caraballo, E., Malone, J., Little, J., Özbay, H., Efe, M. Ö., Yan, P., Yuan, X., DeBonis, J., Myatt, J. H., and Camphouse, R. C., "Exploring Strategies for Closed-Loop Cavity Flow Control," AIAA Paper 2004-0576, January 2004.
28. Samimy, M., Debiasi, M., Caraballo, E., Özbay, H., Efe, M.O., Yuan, X., DeBonis, J., and Myatt, J.H., "Closed-Loop Active Flow Control: A Collaborative Approach," AIAA Paper 2003-0058, 2003.
29. Siegel, S., Cohen, K., Seidel, J., and McLaughlin, T., "Feedback Control of a Circular Cylinder Wake in Experiments and Simulations (Invited)," AIAA Paper 2003-3569, June 2003.
30. Sirovich, L. "Turbulence and the Dynamics of Coherent Structures", *Quarterly of Applied Math*. Vol. XLV, N. 3, 1987, pp. 561-590.
31. Tadmor, G., Noack, B., Morzynski, M., and Siegel, S., "Low-Dimensional Models for Feedback Flow Control. Part II: Control Design and Dynamical Estimation," AIAA Paper 2004-2409, June 2004.
32. Ukeiley, L., and Murray, N., "Velocity and Surface Pressure Measurements in an Open Cavity," *Exp. In Fluids*, Vol. 38, 2005, pp. 656-671.
33. Willcox, K., "Unsteady Flow Sensing and estimation Via the Gappy Proper Orthogonal Decomposition," *Computers & Fluids*, Vol. 35, 2006, pp. 208-226.
34. Williams, D., Fabris, D., and Morrow, J., "Experiments on Controlling Multiple Acoustic Modes in Cavities," AIAA Paper 2000-1903, 2000.
35. Yan, P., Debiasi, D. Yuan, X., Little, J., Özbay, H., and Samimy, M., "Closed-loop Linear Control of Cavity Flow," *AIAA Journal*, Vol. 44, No. 5, pp. 929-938, May 2006.
36. Yuan, X. , Caraballo, E., Yan, P., Özbay, H., Serrani, A., DeBonis, J., Myatt, J. H. and Samimy, M., "Reduced-Order Model-Based Feedback Controller Design for Subsonic Cavity Flows", AIAA Paper 2005-0293, January 2005.

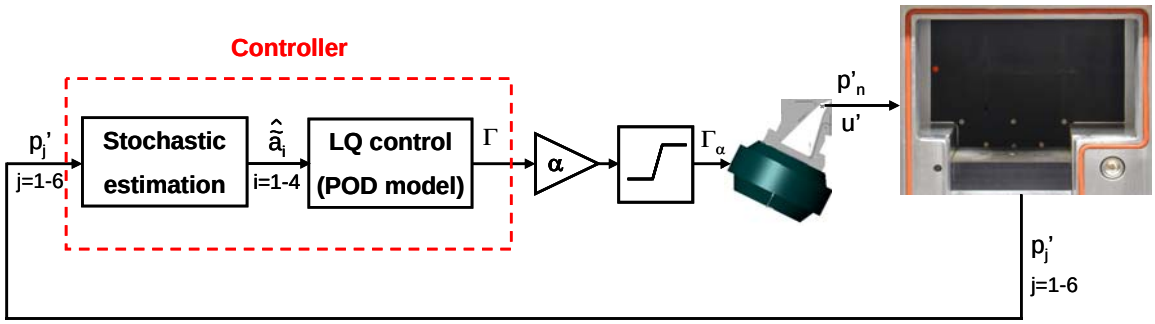

Figure 1 Structure of the model-based controller.

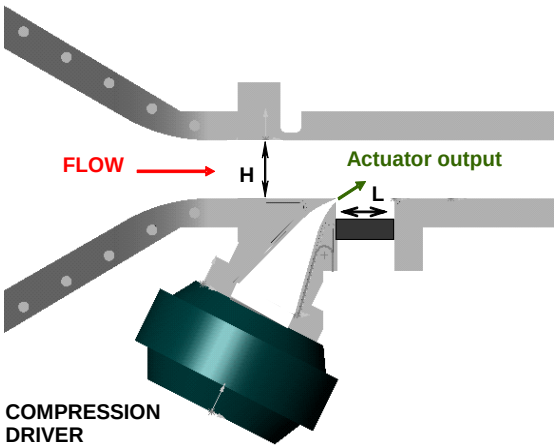

Figure 2 Scaled drawing of the experimental set up showing the test section with the cavity and the actuator.

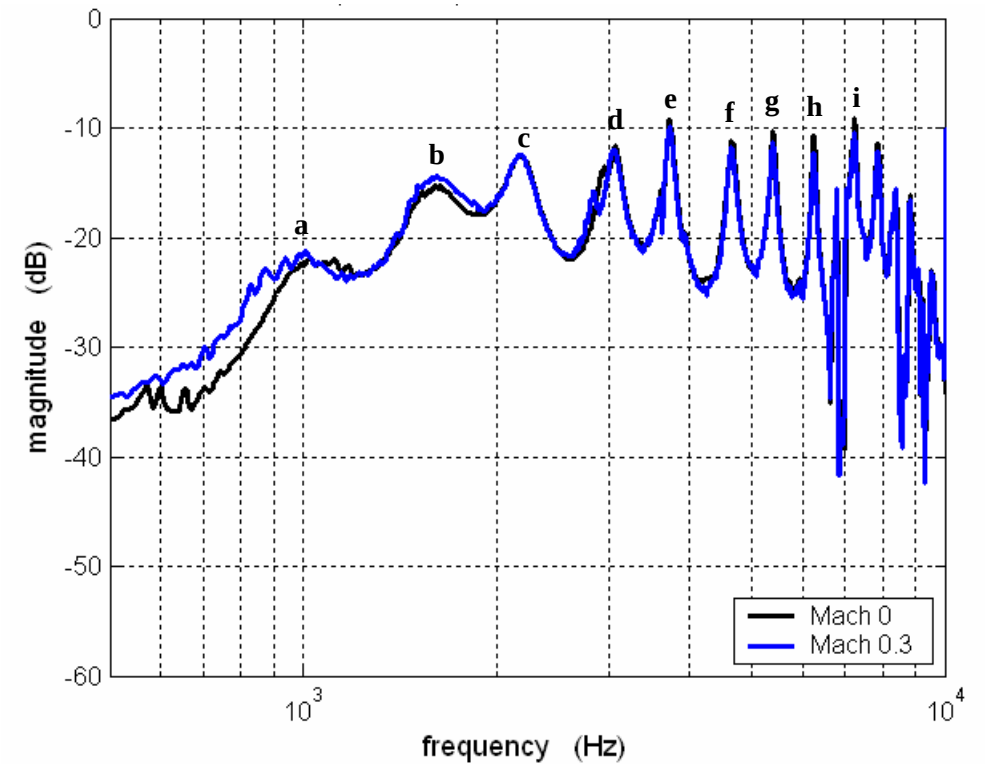

Figure 3 Frequency response of the pressure fluctuations measured immediately upstream the actuator exit slot.

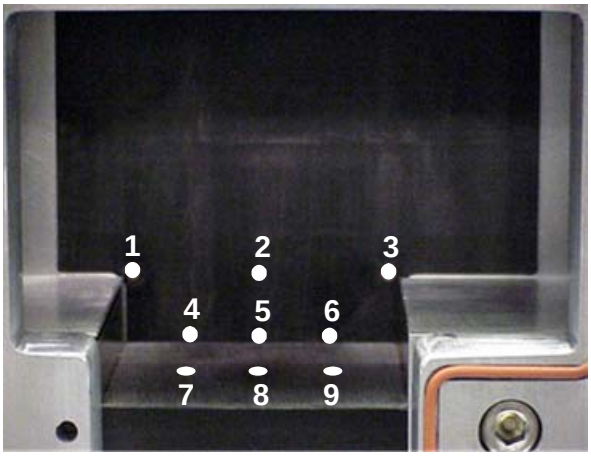

Figure 4 Position of the Kulite pressure transducers in the test section. Transducers 1-6 (on the side wall) were used for cavity flow control.

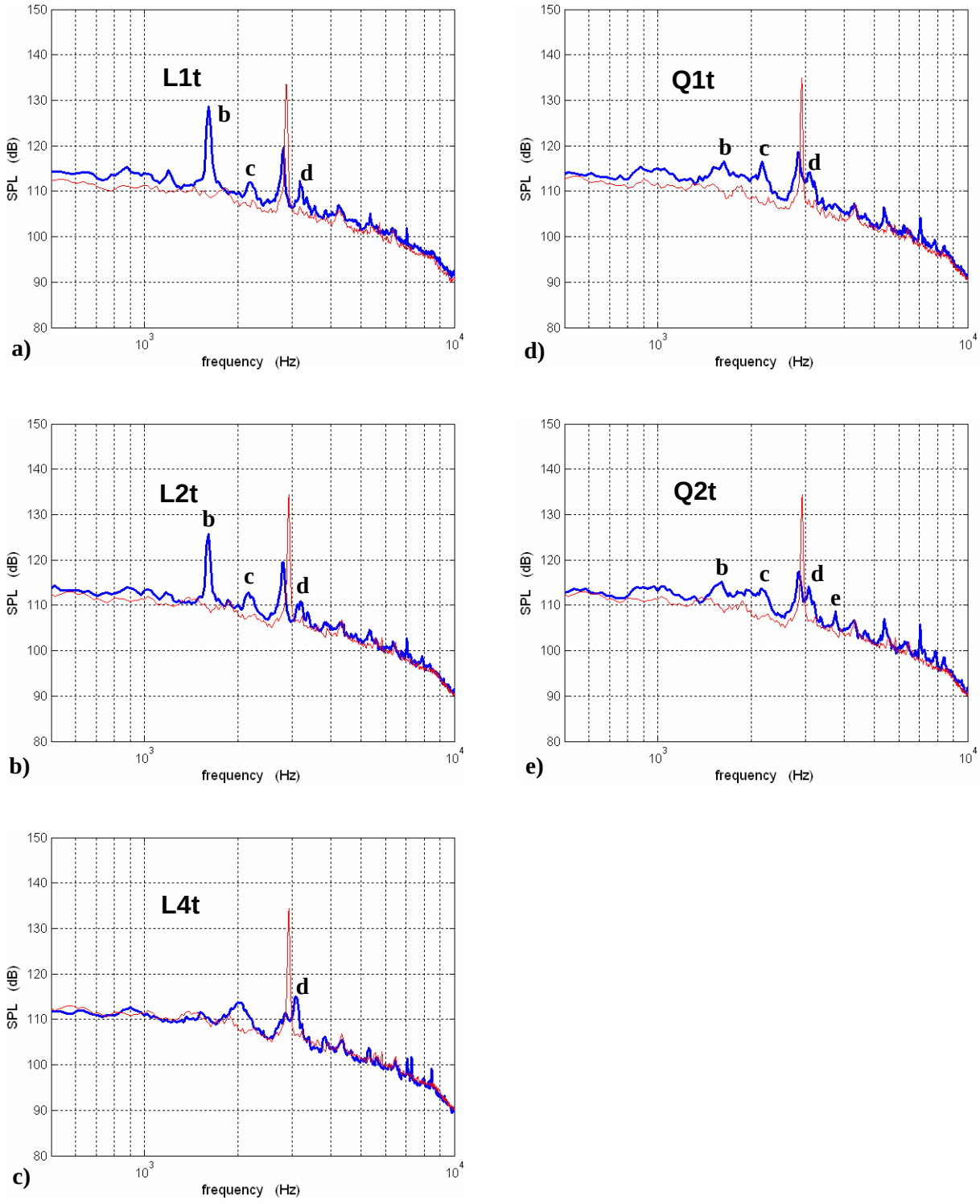

Figure 5 Effect of order and of number of time steps used in the SE for the baseline based controller. Left column is linear SE, right column is quadratic SE. Top is SE with 1 (current) time sample, middle with 2 (current and previous) time sample, bottom with 4 time samples. Red (thin) line is baseline case, blue (thick) line is controlled case.

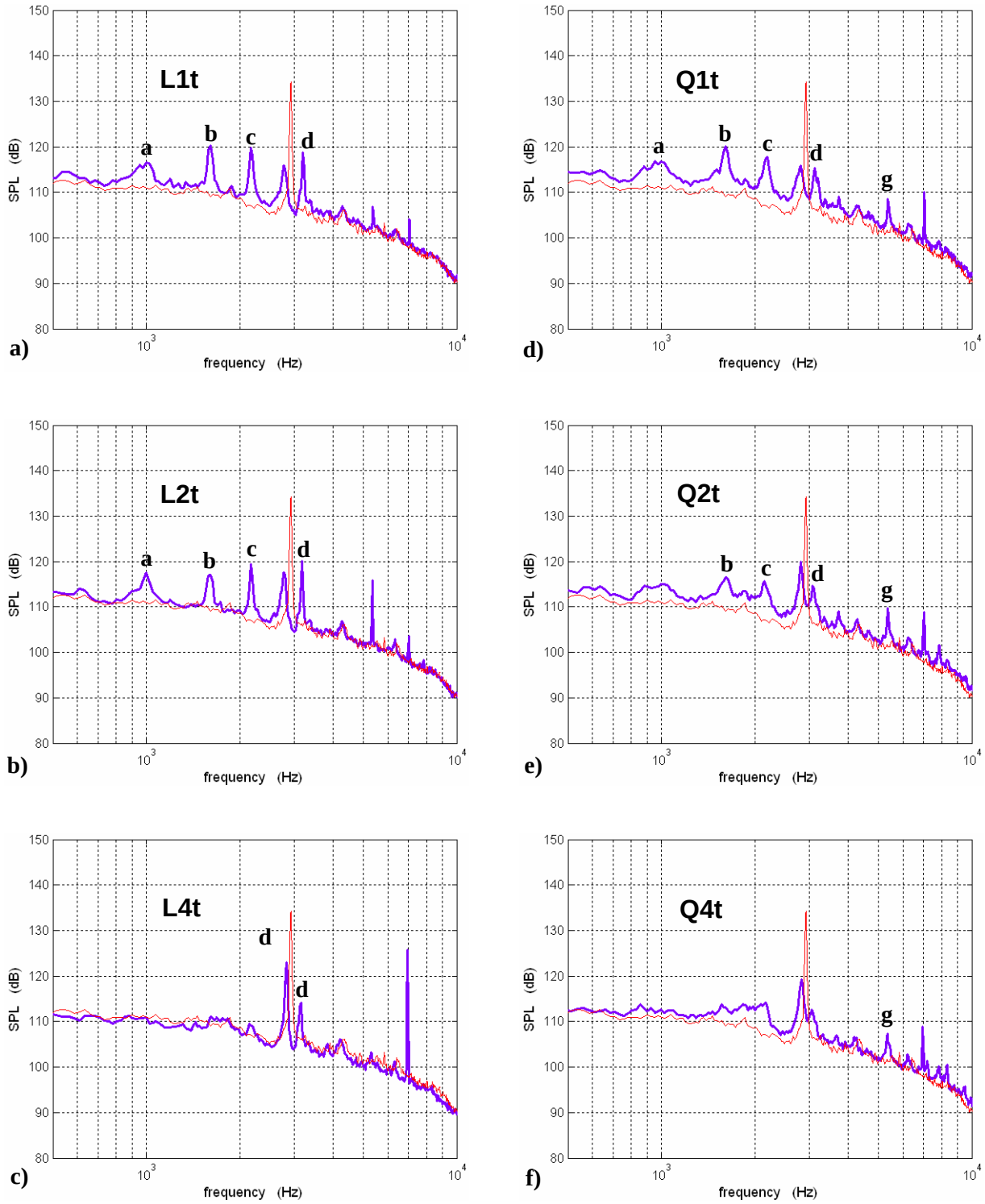

Figure 6 Effect of using a reduced set of pressure signals for SE. Left column is linear SE, right column is quadratic SE. Top is SE with 1 (current) time sample, middle with 2 (current and previous) time sample, bottom with 4 time samples. Red (thin) line is baseline case, purple (thick) line is controlled case.

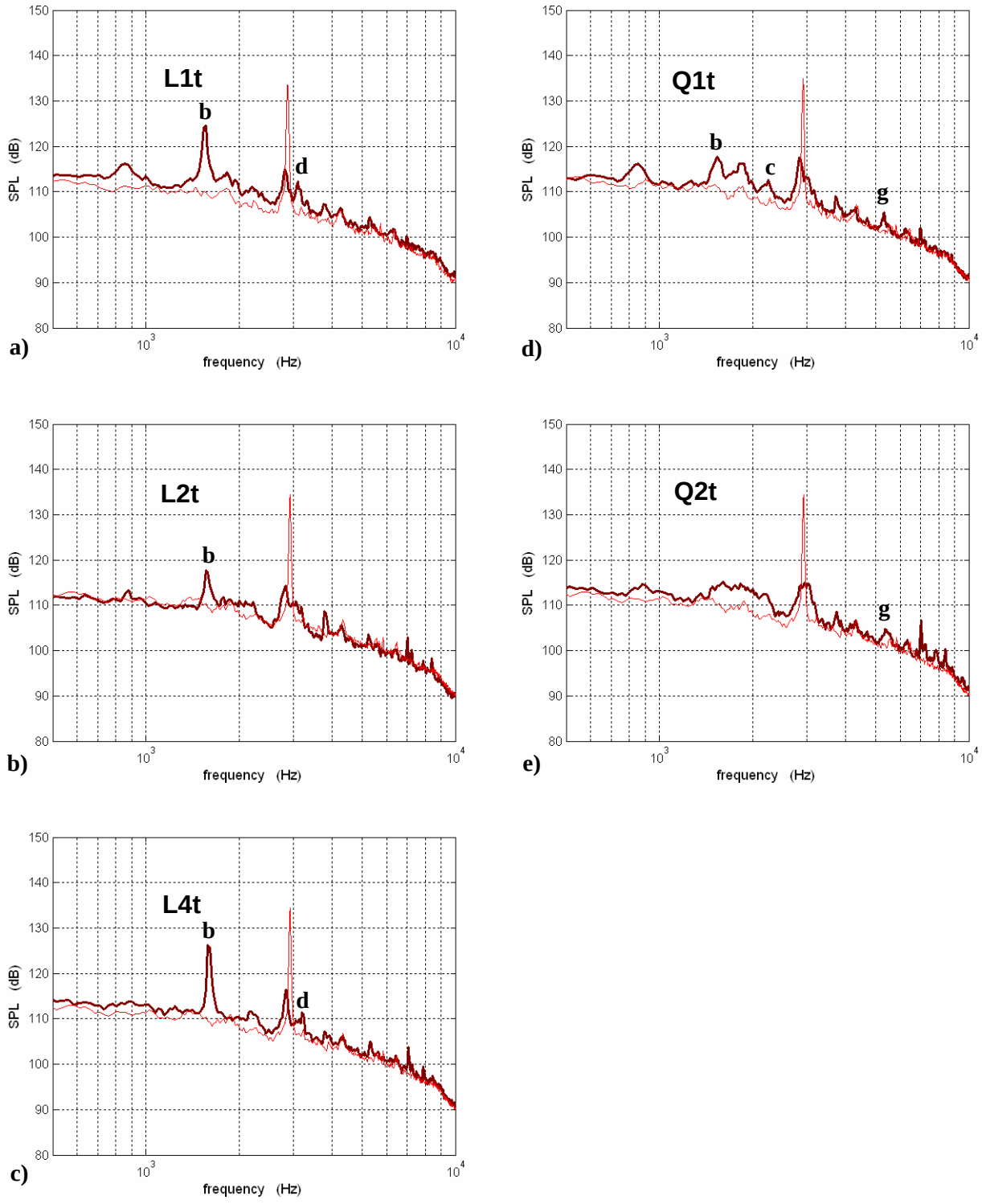

Figure 7 Effect of order and of number of time steps used in the SE for the controller based on combined model of baseline and forced cases. Left column is linear SE, right column is quadratic SE. Top is SE with 1 (current) time sample, middle with 2 (current and previous) time sample, bottom with 4 time samples. Red (thin) line is baseline case, maroon (thick) line is controlled case.